J BONE ONCOL 44 (2024) 100522

Contents lists available at ScienceDirect

Journal of Bone Oncology

journal homepage: www.elsevier.com/locate/jbo

Research Paper

LOX, but not LOXL2, promotes bone metastasis formation and bone destruction in triple-negative breast cancer

Paola Di Mauro [a,b], Martine Croset [a,b], Lamia Bouazza [a,b], Philippe Clézardin [a,b,c,*,1], Caroline Reynaud [a,b,1]

[a] INSERM, UMR1033, F-69372 Lyon, France
[b] University of Lyon, F-69622 Villeurbanne, France
[c] Division of Clinical Medicine, School of Medicine and Population Health, University of Sheffield, Sheffield, UK

HIGHLIGHTS

- LOX (but not LOXL2) promotes breast cancer metastatic osteolytic lesions *in vivo*.
- LOX (but not LOXL2) enhances RANKL-induced osteoclast differentiation *in vitro*.
- LOX (but not LOXL2) induces a robust IL-6 production by tumor cells *in vitro*.

ARTICLE INFO

Keywords:
LOX
LOXL2
Bone
Metastasis
Breast cancer
Osteoclast
Resorption
IL-6

ABSTRACT

The primary function of the lysyl oxidase (LOX) family, including LOX and its paralogue LOX-like (LOXL)-2, is to catalyze the covalent crosslinking of collagen and elastin in the extracellular matrix. LOX and LOXL2 are also facilitating breast cancer invasion and metastatic spread to visceral organs (lungs, liver) *in vivo*. Conversely, the contribution of LOX and LOXL2 to breast cancer bone metastasis remains scant. Here, using gene overexpression or silencing strategies, we investigated the role of LOX and LOXL2 on the formation of metastatic osteolytic lesions in animal models of triple negative breast cancer. *In vivo*, the extent of radiographic metastatic osteolytic lesions in animals injected with LOX-overexpressing [LOX(+)] tumor cells was 3-fold higher than that observed in animals bearing tumors silenced for LOX [LOX(−)]. By contrast, the extent of osteolytic lesions between LOXL2(+) and LOXL2(−) tumor-bearing animals did not differ, and was comparable to that observed with LOX (−) tumor-bearing animals. *In situ*, TRAP staining of bone tissue sections from the hind limbs of LOX(+) tumor-bearing animals was substantially increased compared to LOX(−), LOXL2(+) and LOXL2(−)-tumor-bearing animals, which was indicative of enhanced active-osteoclast resorption. *In vitro*, tumor-secreted LOX increased osteoclast differentiation induced by RANKL, whereas LOXL2 seemed to counteract LOX's pro-osteoclastic activity. Furthermore, LOX (but not LOXL2) overexpression in tumor cells induced a robust production of IL-6, the latter being a pro-osteoclastic cytokine. Based on these findings, we propose a model in which LOX and IL-6 secreted from tumor cells act in concert to enhance osteoclast-mediated bone resorption that, in turn, promotes metastatic bone destruction *in vivo*.

1. Introduction

The lysyl oxidase (LOX) family consists of five secreted copper-dependent amine oxidases with a conserved catalytic domain: LOX and LOX-like 1–4 (LOXL 1–4) [1]. However, the diverse N-terminal propeptide regions of the LOX proteins further divides the family into two subgroups consisting of LOX and LOXL1, and LOXL2-LOXL4. The N-terminal pro-domains of LOX and LOXL1 enable their secretion as

Abbreviations: BLI, bioluminescence imaging; LOX, lysyl oxidase; LOXL2, lysyl oxidase-like 2; M-CSF, macrophage colony-stimulating factor; RANKL, receptor-activated nuclear factor kB ligand.

* Corresponding author at: INSERM, UMR1033, Faculté de Médecine Lyon-Est (domaine Laennec), Rue Guillaume Paradin, 69372 Lyon cedex 08, France.
E-mail addresses: philippe.clezardin@inserm.fr, p.clezardin@sheffield.ac.uk (P. Clézardin), caroline.reynaud@inserm.fr (C. Reynaud).
[1] Last co-authors.

https://doi.org/10.1016/j.jbo.2024.100522
Received 16 May 2023; Received in revised form 22 December 2023; Accepted 3 January 2024
Available online 5 January 2024

inactive pro-enzymes that are then processed by bone morphogenetic protein 1 (BMP1) and BMP1-related proteinases, releasing the catalytically active enzymes and N-terminal pro-domains, whereas LOXL2-LOXL4 are biologically active irrespective of their catalytic activity [1,2]. Furthermore, LOXL2, LOXL3 and LOXL4 contain four scavenger receptor cysteine-rich (SRCR) domains within the N-terminal propeptide region that are thought to be involved in mediating protein–-protein interactions and cell adhesion [1,2].The primary function of the LOX family is to catalyze the covalent crosslinking of collagen and elastin in the extracellular matrix, thereby maintaining extracellular matrix stiffness, which is important for the structural integrity of many tissues during embryonic development and wound healing [1]. Aberrant expression and activity of these proteins have also been reported in human diseases predominantly associated with the dysregulation of matrix homeostasis such as in fibrotic diseases, cardiovascular and neurodegenerative diseases, as well as in malignant diseases (breast, prostate, bladder, renal, colorectal and pancreatic cancer, and melanoma) [1,3].

The evidence that the LOX family of proteins is facilitating cancer progression is compelling [1,3]. In breast cancer, the expression of both *LOX* and *LOXL2* is increased in ER-negative mammary tumors and their upregulation negatively influences overall and metastasis-free survivals in patients with triple negative breast cancer [1,3]. LOX and LOXL2 are upregulated by hypoxia and promote tumor cell invasion and metastasis *in vivo* [1,3–5]. LOX and LOXL2 are also involved in regulating E-Cadherin (CDH1) and vimentin expression, as well as driving epithelial-to-mesenchymal transition (EMT), thereby contributing to the metastatic phenotype of cancer cells [1,3,6]. Inhibiting LOX or LOXL2 by treatment with β-aminopropionitrile (βAPN), function-blocking antibodies, or specific small molecule inhibitors results in the inhibition of lung and liver metastases in xenograft and transgenic mouse models of breast cancer [7–11]. LOX and LOXL2 are also involved in mediating cancer bone metastasis [5,7,8]. For example, we and others have demonstrated that LOX cooperates with receptor activator of nuclear factor-kappaB (RANK) ligand (RANKL) to mediate osteoclast differentiation *in vitro*, which accelerates osteoclastic bone resorption and the formation of metastatic osteolytic lesions in animal models of colon cancer [5,12]. The contribution of LOXL2 to osteoclast differentiation is currently unknown. Furthermore, we do not know whether LOX and LOXL2 have distinct, cooperative, or redundant functions in breast cancer bone metastasis, which may be of importance as the therapeutic targeting of LOX and LOXL2 has potential for the treatment of metastatic disease [1,3,7]. Here, using gene overexpression or silencing strategies, we investigated the role of LOX and LOXL2 on the formation of metastatic osteolytic lesions in animal models of breast cancer.

2. Materials and methods

2.1. Cell culture

Human Hs578T and MDA-MB-231 breast cancer cell lines were obtained from the American Type Culture Collection (Manassas, VA) and authenticated using short tandem repeat analysis. The human MDA-B02 breast cancer cell line (B02) is a subpopulation of the MDA-MB-231 cell line that was selected for its high and selective efficiency to metastasize to bone in mice [13]. MDA-MB-231 and B02 cells were cultured in DMEM medium containing 1.5 g/l glucose (Invitrogen). Hs578T, MCF-7 and T47D cells were cultured in RPMI-1640-Glutamax (Invitrogen). Culture media were supplemented with 10 % (v/v) FBS, and cultured cells maintained in a CO2 incubator at 37 °C. When specified, tumor cells were cultured with 350 μM βAPN (Sigma).

2.2. Plasmid constructs

B02 cells expressing luciferase2 (B02-luc2) were obtained by retroviral transduction of tumor cells with pmiRVec containing the luciferase2 ORF, followed by blasticidin selection [14]. The stable silencing of LOX and LOXL2 was achieved by the RNA interference strategy using lentiviral shERWOORD-UltramiR shARNs vectors (TransOMIC Technologies Inc.). The shRNA sequences predicted by shERWOOD algorithm to target LOX and LOXL2 were inserted in pZIP-hCMV-UltramiRshRNAs vectors optimized with an internal ribosomal entry site and the ZsGreen fluorescente protein. The pZIP-hCMV-UltramiRshCTRL vector was obtained by insertion of the universal non-targeting sequence (Supplementary Table S1).

For the B02-Luc2 cells overexpressing LOX or LOXL2, the LOX and LOXL2 cDNA open reading frame were inserted in the BamH1/EcoR1 restriction site of the retroviral bi-cistronic pQCXN vector (Clontech), by homologous recombination. The LOX cDNA was PCR-amplified from the cloning plasmid pEN-Tmcs-LOX using the PrimeSTAR Max DNA Polymerase Kit and the 5′- and 3′-primers for insertion into the linearized BamH1/EcoR1 PQCXIN using In-Fusion HD Cloning kit (Clontech) (Supplementary Table S2). The LOXL2 cDNA was obtained by RT-PCR amplification of RNA polyA extracted from the Hs578T cell line using the PrimeScript™ High Fidelity RT-PCR kit (Takara) and the 5′- and 3′-primers for insertion into the linearized BamH1/EcoR1 PQCXIN using In-Fusion HD Cloning kit (Supplementary Table S2).

2.3. Cell line engineering

Stable silencing of *LOX* and *LOXL2* was achieved in B02-Luc2, MDA-MB_231 and Hs578T cells by transduction with the lentiviral plasmids containing shRNA hairpins targeting *LOX* and *LOXL2* or a universal negative control using the lentiviral packaging Lenti-X™ Lentiviral Expression System (Clontech Laboratories, Inc, Takara Bio Company, USA). The HEK-293T cell line was cultured in DMEM 4.5 g/l glucose containing 10 % tetracycline-free fetal bovine serum (FBS) (Takara Bio Company, USA) and cells were transfected using a mixture of lentiviral-shRNA plasmids with the Lenti-X HTX Packaging mix in presence of Xfect Polymer diluted in Xfect reaction buffer. After overnight incubation, the transfection medium was removed, and cells were incubated with fresh medium for 48 h prior to supernatant collection. The lentiviral particles filtrated on 0.45 μM pore-size nitrocellulose membranes were incubated with B02-Luc2, MDA-MB_231 and Hs578T cells previously cultured on plates coated with 50 μg/ml Retronectin solution (Takara Bio). The transduced cells were further selected by incubation with medium containing 2 μg/ml puromycin.

Forced expression of *LOX* or *LOXL2* was achieved by retroviral transduction of B02-Luc2 cells using the amphotropic retroviral packaging system (Clontech). Briefly, the GP2-293 cell line expressing viral GAG and POL genes was transfected with the Calcium Phosphate Transfection Kit (CAPHOS, Sigma-Aldrich), using both the pantropic VSV-G vector and one of the bicistronic retroviral expression vector pQCXIN (Clontech). B02-Luc2 cells were incubated with the retroviral particles in the presence of 8 μg/ml polybrene prior to selection with 800 μg/ml neomycin. B02-Luc2 cells overexpressing *LOX* or *LOXL2* were generated by transducing the B02-Luc2-CTRLshLOX and the B02-Luc2-CTRLshLOXL2 with the PQCXIN-LOX and PQCXIN-LOXL2 vectors, respectively, and the mock-transduced B02-Luc2 cells were obtained by transducing the B02-Luc2-shLOX and B02-Luc2-shLOXL2 cells with the PQCXIN-CTRL vector. *LOX* or *LOXL2* silenced cells, and cells overexpressing *LOX* or *LOXL2* were named LOX(−) or LOXL2(−) and LOX(+) or LOXL2(+) for brevity.

2.4. Animal studies

All procedures involving animals, including housing and care, method of euthanasia, and experimental protocols were conducted in accordance with a code of practice established by the local ethical committee (Comité d'Expérimentation Animale de l'Université Claude Bernard Lyon 1, CEEA-55), under project licence DR2018-13. Four-week-old female BALB/c *nude* mice were purchased from Janvier

Laboratories (Saint-Berthevin). BO2 cells +/− LOX or LOXL2 (5.10^5/100 µL of PBS) were inoculated into the tail artery. The progression of the skeletal tumor burden was monitored by whole-body bioluminescence imaging (NightOwl, Berthold Technologies) following subcutaneous administration of luciferin (100 mg/kg in PBS; Promega) 10 min prior to imaging. Signal intensity was quantified as a total of photons/s for a 4-min-period using WinLight software (Berthold Technologies). The progression of osteolytic lesions in the skeleton was determined by radiography/microcomputed tomography (SkyScan 1176, Bruker Biospin). Acquired images were reconstructed using the NRecon software. The area of osteolytic lesions was measured using Explora-Nova Morpho Expert software and the results were expressed in square millimeters. On day 28 after tumor cell inoculation, anesthetized mice were sacrificed by cervical dislocation, and hind limbs were collected and embedded in paraffin for further analyses by histomorphometry, histology, and immunohistochemistry.

2.5. Bone histology and micro-computed tomography (micro-CT)

Histology of bone tissue sections was performed on decalcified, 5-µm bone-tissue sections stained with Goldner's Trichrome, as previously described [15,16]. Micro-CT measurements of bone volume (BV)/tissue volume (TV) were performed in a standard zone of the tibial metaphysis, situated at 0.5 mm from the growth plate, including cortical and trabecular bone using the Burker CTan Micro-CT software. *In situ* bone resorption was measured on tartrate-resistant acid phosphatase (TRAP)-stained medial sections of tibial metaphysis, using a commercial kit (Sigma). Bone resorption (Oc.S/BS) was calculated as the ratio of TRAP-positive trabecular bone surface (Oc.S) to the total bone surface (BS), using the image analysis system ImageJ, as previously described [15,16].

2.6. Real-time quantitative PCR (RT-qPCR)

Total RNA was isolated using the NucleoSpin RNA kit (Machery-Nagel). RNA concentration and purity were measured on Nanodrop ND-1000 (Nanodrop Technologies, Wilmington, DE). First-strand cDNA was synthesized using iScript Reverse-Transcriptase kit (BioRad), according to the manufacturer's instructions. RT-qPCR reactions were performed using a PowerUp SYBER Green Master Mix on QuantStudio 7 (Thermo Fischer Scientific). Relative gene expression levels were normalized according to the C_t value of the gene encoding the ribosomal protein L32 and results were expressed as fold differences equal to $2^{-\Delta\Delta Ct}$. Sequences for primer pairs are listed in Supplementary Table S3.

2.7. Protein extraction and Western blotting

Proteins were extracted with RIPA buffer containing protease inhibitors, and concentration was determined using the BCA assay (Pierce). Whole-cell extracts were resolved by SDS-PAGE, probed with a specific primary antibody, and revealed with the enhanced chemiluminescence system (Pierce). Quantifications were made using the Quantity One software (Bio-Rad). Antibodies used were as follow: LOX (ab3128, 1/1,000 dilution, Abcam); LOXL2 (ab96233, 1:1,000 dilution, Abcam); tubulin (T5168, 1:2,000 dilution, Sigma); HRP-conjugated secondary goat anti-mouse (1:2,000 dilution, BioRad), and HRP-conjugated secondary goat anti-rabbit (1:2,500 dilution, BioRad).

2.8. Conditioned media

For experiments conducted with the conditioned media from cells in culture, $4x10^6$ cells/ml B02 [Ctrl, LOX(+), LOX(−), LOXL2(+) and LOXL2(−)], or MDA-MB-231 and Hs 578T cells [Ctrl, LOX(−) and LOXL2(−)] treated or not treated with 350 µM βAPN were cultured for 48 h in phenol red-free DMEM or RMPI medium supplemented with 0.5 % (v/v) FCS. Conditioned media were then collected, centrifuged, and stored as aliquots at −80 °C.

3. Lysyl oxidase activity assay

The assay was performed according to the manufacturer instructions (ab112139 Abcam). Briefly, 50 µL of cell conditioned media, or increasing concentrations of recombinant LOX (Creative Biomart) were mixed with HRP substrate and horseradish peroxidase in a black 96-well plate. After a 30 min incubation at 37 °C in dark, fluorescence was read at 590 nm.

3.1. Functional cell-based assays

Cell migration assays were performed as previously described [15], using porous membrane inserts with 8 µm pores (Corning) for 24-well plates. Briefly, cells (3×10^4 cells/0.3 ml/well) were resuspended in serum-free DMEM or RPMI medium and applied to the upper compartment of *trans*-well inserts. As a chemoattractant, 0.5 ml of DMEM or RMPI medium supplemented with 10 % FBS was used in the lower compartment. Cells were allowed to migrate for 24 h, then cells in the upper chamber were removed using a cotton swab. The cells that had migrated to the other side of the membrane were fixed with 70 % (v/v) ethanol for 15 min, then stained with a 0.5 % (w/v) crystal violet solution in distilled water. The dye was eluted with 2 % (w/v) SDS and the optical density quantified at 570 nm.

Cell adhesion assays were conducted in 96-well tissue culture plates, as previously described [5]. Culture plates were coated with type-I collagen or fibronectin (15 µg/cm^2) and incubated at 4 °C overnight. Before use, coated wells were overlaid with 1 % (w/v) BSA for 30 min and washed with PBS. Cells (1×10^5 cells/0.1 ml/well) were allowed to adhere for 1 h at 37 °C in a 5 % CO_2 atmosphere. Adherent cells were then fixed for 30 min in 2.5 % (v/v) paraformaldehyde and stained with crystal violet 0.1 %(w/v). The dye was eluted with 2 % (w/v) SDS and the optical density quantified at 570 nm.

For cell proliferation assays, cells were grown in 96-well tissue culture plates (1×10^5 cells/0.1 ml/well) with BrDU for 16 h. BrDU incorporation into newly synthesized DNA was measured according to the manufacturer's instructions using an anti-BrDU antibody (Cell Proliferation ELISA, BrDU colorimetric, Merck). All experiments were performed three times in quadruplicate.

3.2. Osteoclastogenesis assay

Experiments were conducted using bone marrow cells from 6-weeks-old OF1 male mice cultured for up to 7 days in α-MEM medium (Invitrogen) supplemented with 10 % (v/v) FCS (Invitrogen), 20 ng/ml macrophage colony-stimulating factor (M-CSF; R&D Systems), and 5 ng/ml RANKL, as previously described [5]. Cells were either exposed for 4 or 7 days (from day 1 to 4 or day 1 to 7) to the conditioned medium (25 µg proteins) from B02 Ctrl, LOX(+), LOX(−), LOXL2(+) and LOXL2(−) cells +/− βAPN, or MDA-MB-231 and Hs578T Ctrl, LOX(−) or LOXL2 (−) cells. After 4 or 7 days, multinucleated osteoclasts were stained for TRAP activity (Sigma) and counted under a microscope based on the number of nuclei (more than three nuclei).

3.3. ELISA assays

Conditioned media from B02, Ctrl, LOX(+), LOX(−), LOXL2(+) and LOXL2(−) cells were collected and IL-6 levels measured by ELISA, according to the manufacturer's instructions (Sigma-Aldrich).

Clinical correlation analyses. Gene expression data and clinical annotations were downloaded from The Cancer Genome Atlas (TCGA) for breast cancer and previously published datasets were downloaded from the Gene Expression Omnibus (GSE2034).

Statistical analysis. All experimental data are presented as mean values ± SD. Statistical comparisons of values were made using the

Mann-Whitney *U* test. Correlation analyses were performed by the Pearson r test. All tests were two-sided, and *P* values less than 0.05 were considered statistically significant.

4. Results

4.1. LOX and LOXL2 are highly expressed in human estrogen receptor (ER)-negative breast cancer cells

To compare the role of LOX and LOXL2 in breast cancer bone

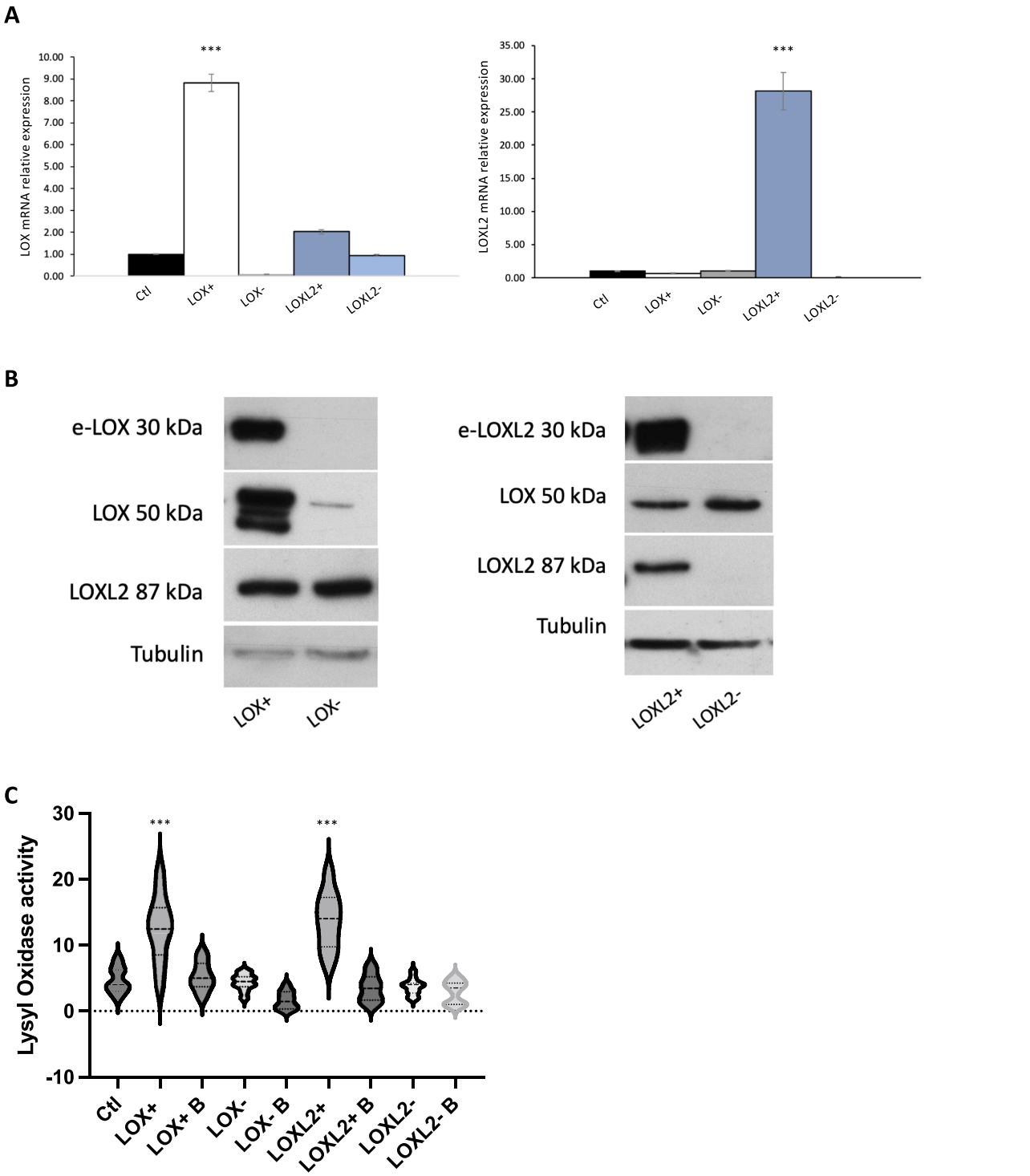

Fig. 1. . Characterization of human B02 breast cancer cells for LOX and LOXL2 expression. (A) LOX and LOXL2 mRNA levels were quantified by RT-qPCR in mock-transduced (Ctrl), *LOX- or LOXL2*-overexpressed [LOX(+), LOXL2(+)] or silenced [LOX(−), LOXL2(−)] B02 cells. Relative gene expression levels were normalized according to the C_t value of the gene encoding the human ribosomal protein L32. (B) Immunoblot analysis of total and extracellular (e−) LOX and LOXL2 in B02 LOX (+), LOX(−), LOXL2(+) and LOXL2(−) cells. Tubulin was used as a control for equal loading. (C) Lysyl oxidase enzymatic activity was measured in the conditioned media from B02 LOX(+), LOX(−), LOXL2(+) or LOXL2(−) cells, treated or not treated with βAPN (B), using a fluorometric assay. Data are the mean ± SD of three independent experiments. ***: $p < 0.001$.

metastasis, we first examined their respective expression levels in various human breast cancer cell lines. As previously reported by Kirschmann *et al.* [17], *LOX* and *LOXL2* were highly expressed in metastatic ER-negative breast cancer cells (MDA-MB-231, Hs578T), including the osteotropic MDA-MB-231 cell subpopulation B02, compared to their poorly invasive ER-positive counterparts (MCF-7 and T47D) (Supplementary Fig. S1). Their high expression levels in ER-negative breast cancer cells were also associated with low E-cadherin levels, and high N-cadherin levels in ER-negative Hs578T cells (Supplementary Fig. S1).

LOX or *LOXL2* expression was then either silenced or overexpressed in human B02 breast cancer cells. Silencing and overexpression efficiencies were examined by RT-qPCR and Western blotting, the latter being conducted both on cell extracts and conditioned media. *LOX* overexpression or silencing did not affect endogenous *LOXL2* expression levels in B02 cells (Fig. 1A-B). Similarly, *LOX* endogenous levels remained unchanged when *LOXL2* was overexpressed or silenced in these cells (Fig. 1A-B). In addition, the modulation of *LOX* and *LOXL2* did not affect the expression of other LOX-like family members (Supplementary Table S4). Furthermore, the lysyl oxidase activity of the conditioned medium from βAPN-treated B02 LOX(+) and LOXL2(+) cells was substantially reduced compared to that observed with untreated cells (Fig. 1C), demonstrating that LOX and LOXL2 produced by these cells were both enzymatically active.

4.2. Tumor-secreted LOX, but not LOXL2, promotes the formation of osteolytic lesions in tumor-bearing animals

In vitro, the modulation of LOX or LOXL2 expression in B02 breast cancer cells did not affect the ability of tumor cells to proliferate, migrate or to adhere on connective substrates such as type-I collagen or fibronectin (Supplementary Fig. S2A-C). *In vivo*, subcutaneous injection of B02 LOX(+) cells led to the growth of tumors in animals that were comparable in size and weight to subcutaneous tumors from animals inoculated with B02 LOX(−) cells. The size and weight of subcutaneous tumors from animals injected with B02 LOXL2(+) or LOXL2+(−) cells were also similar (Supplementary Fig. S2D).

We next investigated the role(s) of LOX and LOXL2 in an animal model of bone metastasis where human B02 cells were injected intra-arterially to immunocompromised mice. Pilot experiments were first

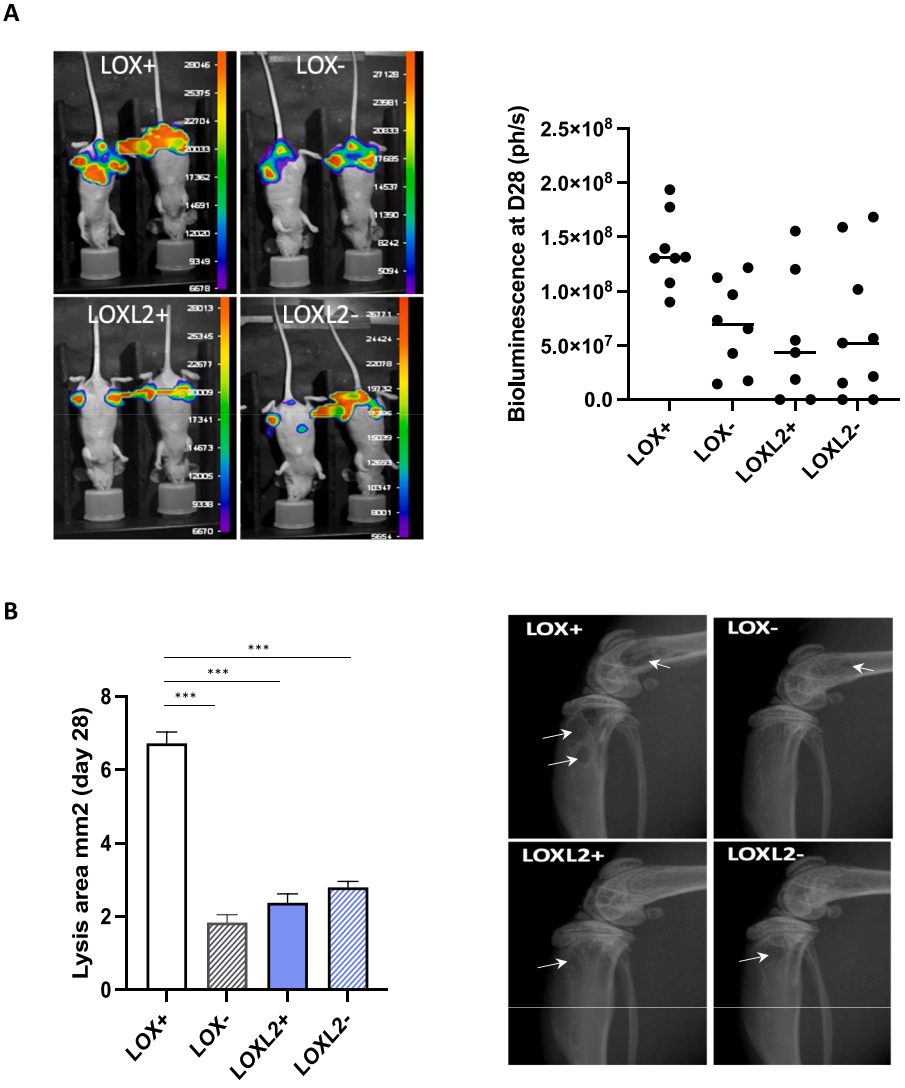

Fig. 2. High LOX expression in human breast cancer cells promotes the formation of metastatic osteolytic lesions *in vivo*. (A) Whole body bioluminescence imaging of animals and quantification of bioluminescence (photon/s) at day 28 after intra-arterial inoculation of luciferase2-expressing B02 LOX(+), LOX(−), LOXL2(+) or LOXL2(−) cells. *Left-hand panels*: Images that best illustrate data obtained for each group (n = 7 to 9 per group). (B) Quantification of osteolytic lesions areas (mm^2) on radiographs at day 28 after intra-arterial inoculation of B02 LOX(+), LOX(−), LOXL2(+) or LOXL2(−) cells. *Right-hand panels*: Radiographs that best illustrate data obtained for each group. Arrows indicate osteolytic lesions. ***: $p < 0.001$.

conducted to quantify the extent of osteolysis in animals inoculated with B02 LOX(−) or LOXL2(−) tumor cells compared with that observed for animals inoculated with B02 parental (Ctrl) tumor cells (Supplementary Fig. S3A). No difference in the extent of bone destruction was observed between LOX(−), LOXL2(−) and Ctrl tumor-bearing animals (Supplementary Fig. S3A). In the light of these findings and to limit the number of animals to be used for additional bone metastasis experiments, we chose to use LOX(−) and LOXL2(−) tumor-bearing mice as the respective negative controls of LOX(+) and LOXL2(+) tumor-bearing animals. Bone metastasis formation is monitored weekly by bioluminescence imaging (BLI) and radiography of animals to measure the extent of tumor burden and bone destruction, respectively (Supplementary Fig. S3B and Fig. 2). Compared to LOX(−) tumor-bearing animals, the extent of tumor burden was increased two-fold in the hind limbs of animals bearing LOX(+) tumors at day 28 post injection (Fig. 2A). By contrast, the tumor burden between LOXL2(+) and LOXL2(−) tumor-bearing animals did not differ, and its extent was comparable to that observed with LOX(−) tumor-bearing animals (Fig. 2A). The extent of osteolytic lesions in LOX(+) tumor-bearing animals was also 3-fold higher than that observed for animals bearing LOX(−), LOXL2(+) or LOXL2(−) tumors (Fig. 2B). Furthermore, the incidence of radiographic osteolytic lesions in animals injected with LOX(+) tumor cells was twice as high as that observed in LOX(−) tumor-bearing animals (100 and 50 %, respectively) (Supplementary Fig. S3C), whereas all the animals from both groups were bearing tumors in hind limbs, as judged by BLI (Fig. 2A). With regard to LOXL2, the incidence of osteolytic lesions in LOXL2(+) and LOXL2(−) tumor-bearing animals varied from 55 to 57 %, whereas 71 to 77 % of animals were BLI-positive (Supplementary Fig. S3C). Micro-CT analysis of hind limbs with metastases from animals bearing B02 tumors was also conducted to measure the bone volume. The BV/TV ratio (as a measure of the bone volume) was substantially decreased in LOX(+) tumor-bearing animals, compared to that observed with LOX(−), LOXL2(+) and LOXL2(−) tumor-bearing animals (Fig. 3A). This difference was accompanied with a sharp increase in

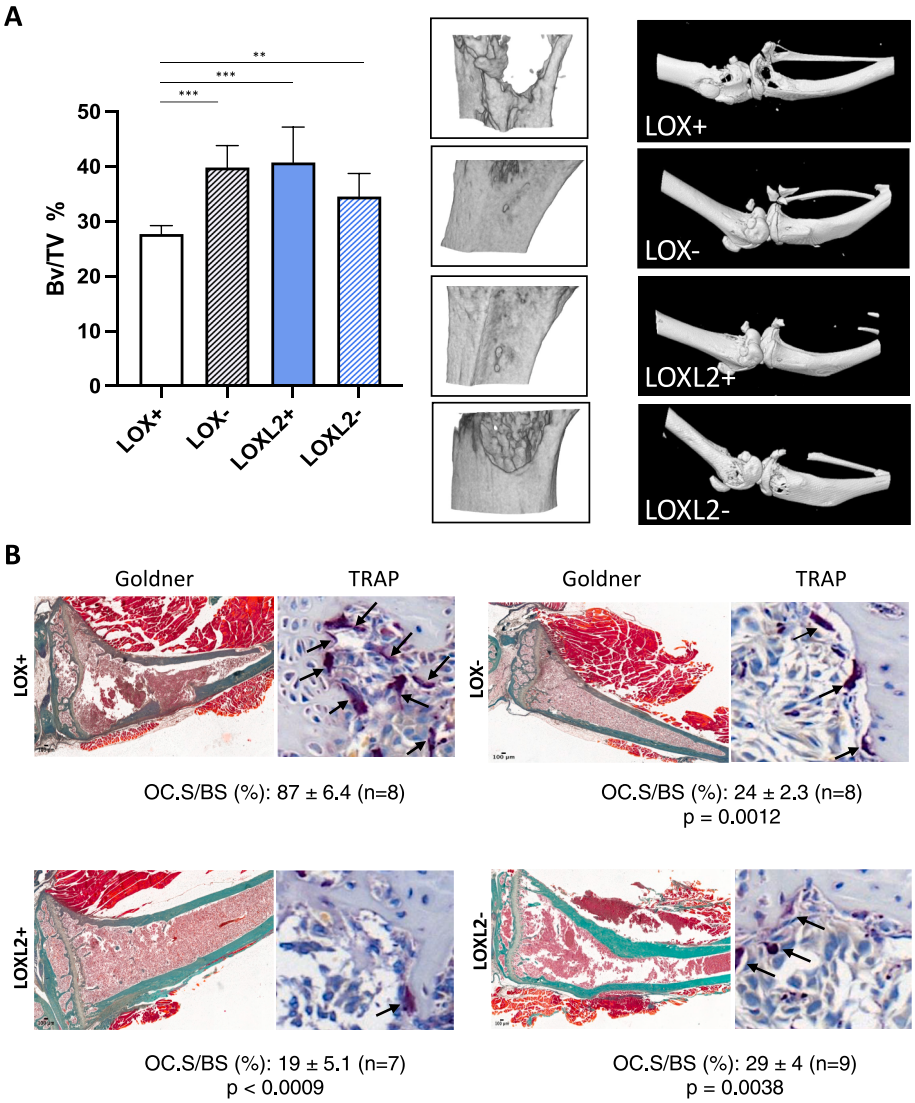

Fig. 3. High LOX expression in human breast cancer cells promotes osteoclast-mediated bone destruction *in situ*. (A) *Left-hand panel*: Graphs showing the micro-CT quantification of the Bone Volume/Tumor Volume (BV/TV, %) at day 28 after intra-arterial inoculation of B02 LOX(+), LOX(−), LOXL2(+) or LOXL2(−) cells. *Middle panels*: 3-D cross sectional tibial metaphysis area which the BV/TV data was captured from. *Right-hand panels*: 3-D whole micro-CT images of hind limbs that best illustrate data obtained for each group. (B) Goldner's trichrome staining of tissue sections of tibial metaphysis from animals inoculated with B02 LOX(+), LOX(−), LOXL2(+) or LOXL2(−) cells. Bone is stained green whereas bone marrow and tumor cells are stained red. Alternatively, metastatic bone tissue sections were stained for TRAP, enabling the detection of osteoclasts (black arrows). All images were obtained from different mice at day 28 after tumor cell inoculation. Images shown are examples that best illustrate LOX's and LOXL2's effects on tumor burden (Goldner) and osteoclast-mediated bone resorption (TRAP). OC.S/BS (%): percentage of active osteoclast-resorption surface per trabecular bone surface. Data are the mean ± SD. *p* values for pairwise comparison with the LOX(+) group are indicated.

skeletal tumor burden, as judged by Goldner staining of bone tissue sections of metastatic legs from LOX(+) tumor-bearing animals (Fig. 3B). In addition, there was a 3- to 4-fold increased TRAP staining, indicating an enhancement of active-osteoclast resorption surfaces on these bone tissue sections of metastatic legs from animals bearing LOX (+) tumors (Fig. 3B).

Taken together, these results indicated that, irrespective of their growth properties, LOX-overexpressing tumor cells were more prone to induce osteolytic lesions in animals compared to LOX(−), LOXL2(+) and LOXL2(−) tumor cells.

4.3. *LOX, but not LOXL2, enhances bone resorption by stimulating osteoclastogenesis*

To directly test whether *LOX* or *LOXL2* expression in B02 cells could influence osteoclast differentiation, we treated primary mouse bone marrow cells in culture with RANKL and M-CSF together with the conditioned medium derived from B02 LOX(+), LOX(−), LOXL2(+) or LOXL2(−) cells. Consistent with *in vivo* data (Fig. 3B), the B02 LOX(+) cell-conditioned medium stimulated by almost 3-fold the formation of TRAP-positive multinucleated osteoclasts after 4 days in culture, when compared to that observed with the conditioned medium from B02 LOX (−) cells (Fig. 4A-B). Specifically, the B02 LOX(+) cell-conditioned medium enhanced the formation of osteoclasts with more than 10 nuclei (Supplementary Fig. S4), the latter being those that are the most active to resorb bone [17]. By contrast, the pro-osteoclastic effects of B02 LOXL2(+) and LOXL2(−) cell-conditioned media did not significantly differ from each other, and were similar to that observed with the B02 LOX(−) cell-conditioned medium (Fig. 4A-B). Additionally, βAPN treatment, that almost completely inhibited lysyl oxidase enzymatic activity in B02 LOX(+) and LOXL2(+) cell-conditioned media (Fig. 1C), only significantly blocked the stimulatory effect of LOX on osteoclast differentiation (Fig. 4A-B). There was just a modest reduction of the pro-osteoclastic effects of B02 LOXL2(+) and LOXL2(−) cell-conditioned media upon βAPN treatment, which was probably due to the inhibition of endogenous LOX activity in these cells (Fig. 4A-B). After 7 days of treatment with the conditioned medium, the total number of osteoclasts reached a plateau, irrespective of the presence or absence of LOX or LOXL2 (Fig. 4C-D). However, in the presence of B02 LOX(+) conditioned medium, there was a high number of osteoclast ghosts at day 7 (these are apoptotic osteoclasts which are distinguishable by their silhouette) (Fig. 4C). In general, when using an assay to differentiate osteoclasts from the bone marrow of mice, osteoclasts suddenly appear at day 6 or 7 of culture and then rapidly undergo apoptosis after 10 days

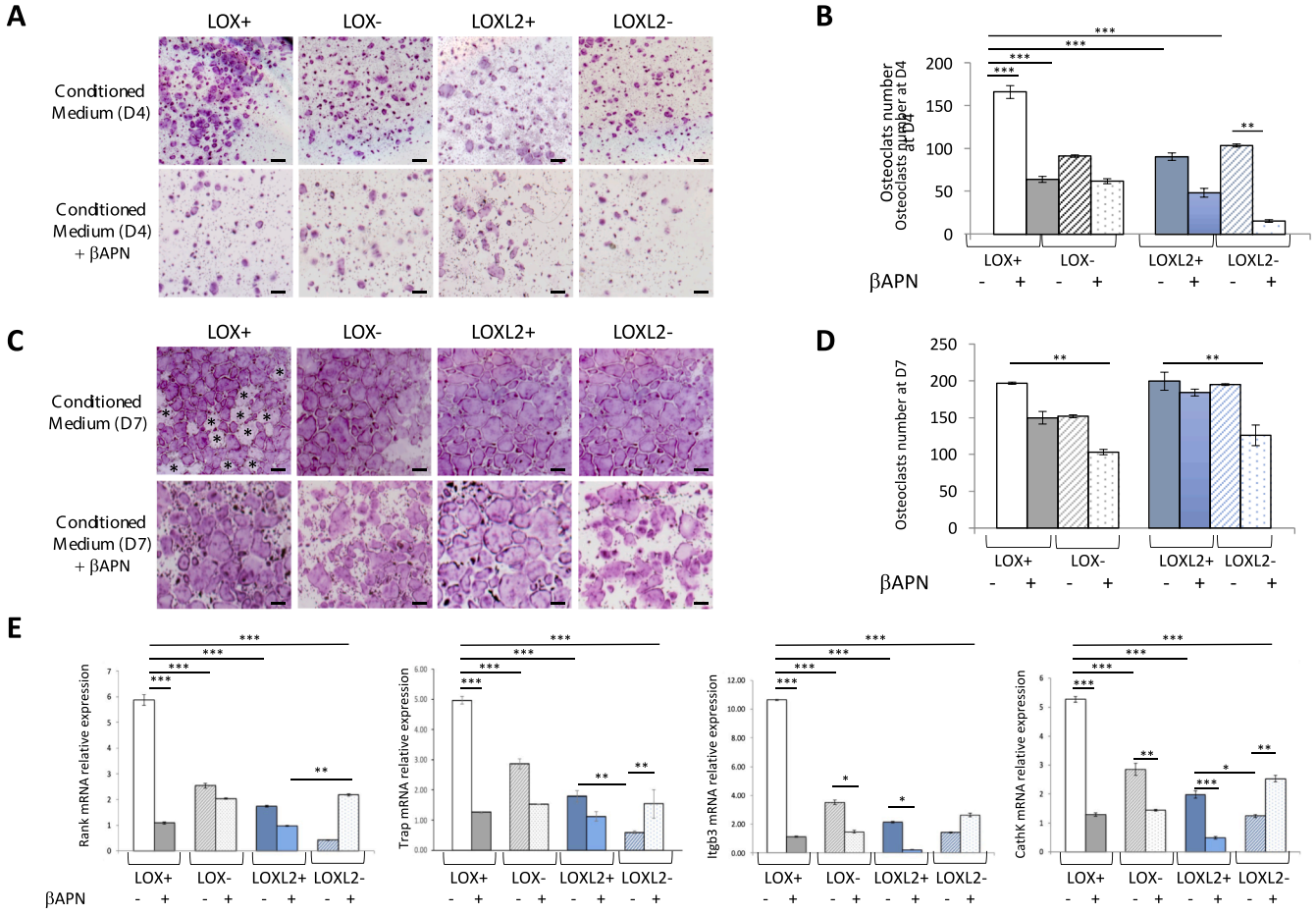

Fig. 4. Tumor-derived LOX stimulates osteoclastogenesis. *In vitro* osteoclast differentiation of murine bone marrow cells treated with M-CSF + RANKL in combination with the conditioned medium from +/− βAPN-treated B02 LOX(+), LOX(−), LOXL2(+) or LOXL2(−) cells. (A) TRAP staining of differentiated osteoclasts at day 4 in culture. Images shown are examples that best illustrate data obtained for each group. (B) Mature osteoclasts at day 4 in culture were quantified as multinucleated (more than 3 nuclei) TRAP-positive cells. (C) TRAP staining of differentiated osteoclasts at day 7 in culture. Images shown are examples that best illustrate data obtained for each group. *: osteoclast ghosts; apoptotic osteoclasts which are distinguishable by their silhouette. (D) Quantification of mature osteoclasts at day 7 in culture. (E) Quantitative PCR determination of the relative levels of *Rank*, *Trap*, *integrin β3* (*Itgb3*) and *cathepsin K* (*CathK*) in murine bone marrow cells treated for 4 days with M-CSF + RANKL and the conditioned medium from +/− βAPN-treated B02 LOX(+), LOX(−), LOXL2(+) or LOXL2(−) cells. Relative gene expression levels were normalized according to the C_t value of the gene encoding the mouse ribosomal protein L32. Data are the mean ± SD of three independent experiments. *, **, ***: $p < 0.05$, 0.01 and 0.001, respectively. Scale bar: 250 μM.

in culture, leaving recognizable « ghosts » [18]. Here, osteoclast differentiation was accelerated in the presence of LOX and therefore reached a plateau early compared to that observed with LOX(−), LOXL2 (+) and LOXL2(−) conditioned media (Fig. 4A-B), thereby explaining the presence of numerous apoptotic osteoclasts after 7 days in culture (Fig. 4C).

To better understand the functional difference between LOX and LOXL2 on osteoclast-mediated bone resorption, we then examined mRNA expression levels of markers associated with osteoclast differentiation at day 4 of culture. The pro-osteoclastic effect of the conditioned medium from B02 LOX(+) cells on osteoclastogenesis was accompanied by a substantial increase of *Rank* and Trap (two markers associated with osteoclast differentiation), itgb3 (integrin beta3, a marker associated with cytoskeleton morphology) and cathK expression (cathepsin K, a cysteine protease enabling collagenous matrix degradation) (Fig. 4E). As expected, the expression of theses markers was abrogated when using the conditioned medium from βAPN-treated B02 LOX(+) cells (Fig. 4E). By contrast, the LOXL2(+) cell-conditioned medium only weakly increased expression levels of *Rank*, *Trap*, *itgb3*

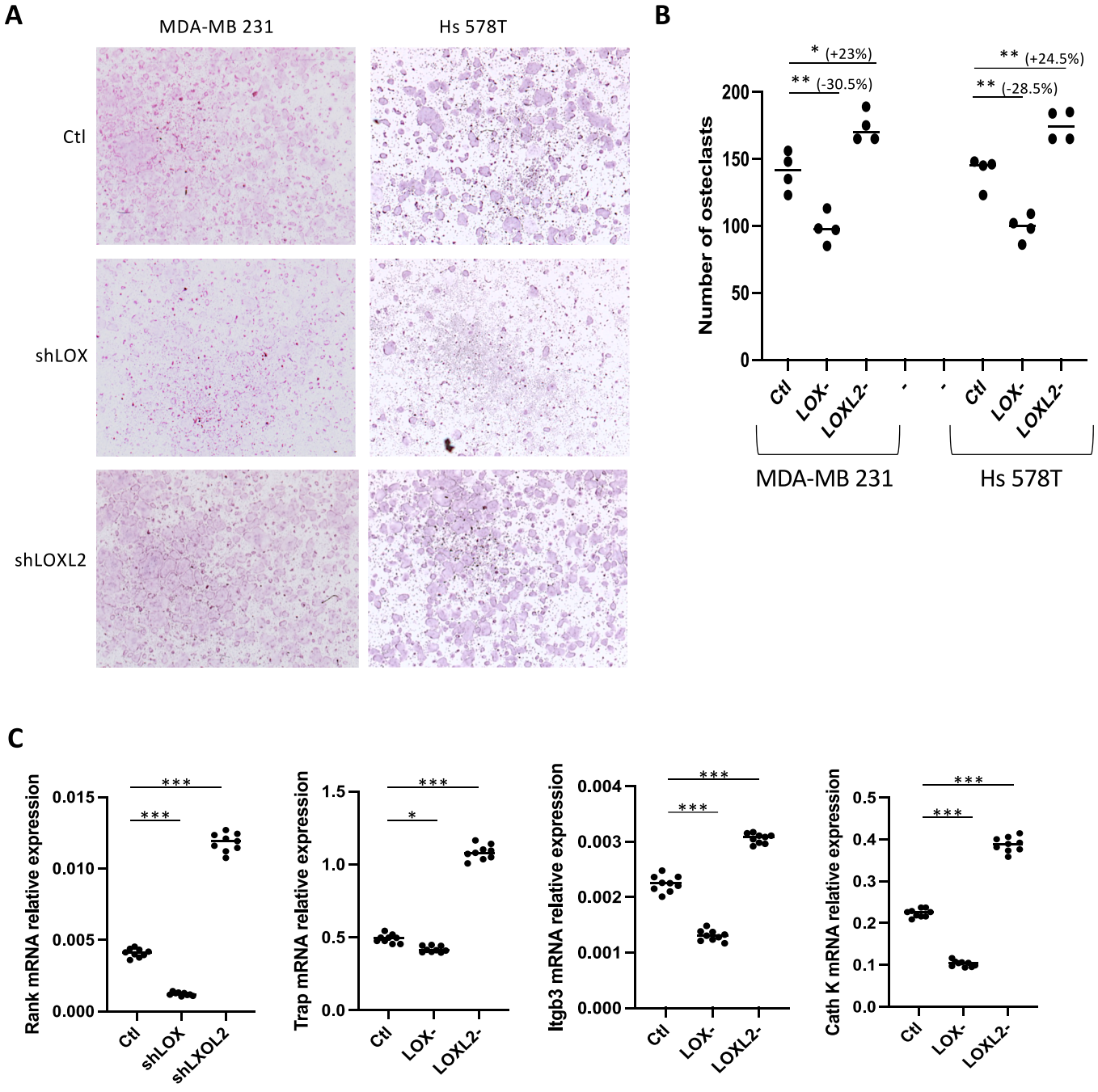

Fig. 5. LOX inhibition impairs osteoclast differentiation induced by human MDA-MB 231 and Hs 578T breast cancer cells. *In vitro* osteoclast differentiation of murine bone marrow cells treated with M-CSF + RANKL in combination with the conditioned medium from MDA-MB 231 or Hs 568T Ctrl, LOX(−) or LOXL2(−) cells. (A) TRAP staining of differentiated osteoclasts at day 7 of culture. Images shown are examples that best illustrate data obtained for each group. (B) Mature osteoclasts were quantified as multinucleated (more than 3 nuclei) TRAP-positive cells (n = 4). (C) Quantitative PCR determination of the relative levels of *Rank*, *Trap*, *integrin* β*3* (*itgb3*) and *cathepsin K* (*cathK*) in murine bone marrow cells treated for 7 days with M-CSF + RANKL and the conditioned medium from MDA-MB 231 Ctrl, LOX(−), or LOXL2(−) cells (n = 9). Relative gene expression levels were normalized according to the C_t value of the gene encoding the mouse ribosomal protein L32 *, **, ***: $p < 0.05$, 0.01 and 0.001, respectively.

and *cathK,* compared to that observed with the conditioned medium from LOXL2(−) cells, and this modest stimulatory effect was inhibited following βAPN treatment of B02 LOXL2(+) cells (Fig. 4E).

To show that our results were not restricted to B02 cells, we then performed additional osteoclastogenesis experiments using human MDA-MB-231 and Hs578T breast cancer cells in which *LOX* or *LOXL2* expression was stably silenced. We chose to silence *LOX* or *LOXL2* because they were both highly expressed in these breast cancer cell lines (Supplementary Fig. S1). The silencing of *LOX* in MDA-MB-231 and Hs578T cells did not affect endogenous *LOXL2* levels. Similarly, endogenous *LOX* levels remained unchanged following *LOXL2* silencing (Supplementary Fig. S5A-B). Moreover, *LOX* or *LOXL2* silencing did not modify proliferative, migratory, and adhesive properties of transduced MDA-MB-231 and Hs578T cells (Supplementary Fig. S5C-F). However, compared to the conditioned medium from MDA-MB-231 and Hs578T control cells, *LOX* silencing in both cell lines partially impaired the pro-osteoclastic effect of the conditioned media derived from these cancer cells (30 % inhibition) (Fig. 5A-B). This inhibitory effect was confirmed by measuring mRNA expression levels of markers associated with osteoclast differentiation (Fig. 5C). Surprisingly, there was a statistically significant enhancement of osteoclast differentiation in the presence of the conditioned medium from MDA-MB-231 LOXL2(−) or Hs578T LOXL2(−) cells (Fig. 5A-B). Accordingly, the MDA-MB-231 LOXL2(−) cell-conditioned medium significantly increased expression levels of osteoclastic markers when compared to that observed with the control medium (Fig. 5C).

Overall, these results showed that LOX overexpression and LOXL2 silencing promoted osteoclast differentiation induced by RANKL and M-CSF.

4.4. *LOX, but not LOXL2, drives IL-6 production by human breast cancer cells*

LOX overexpression induced a robust secretion of IL-6 from B02 breast cancer cells, whose production was inhibited by βAPN treatment (Fig. 6A). Conversely, *LOX* silencing in B02 cells substantially reduced IL-6 production (Fig. 6A). By contrast, the overexpression or silencing of *LOXL2* did not have any effect on IL-6 production by B02 cells (Fig. 6A). Similar experiments were conducted with MDA-MB-231 breast cancer cells in which *LOX* silencing led to a more robust reduction of IL-6

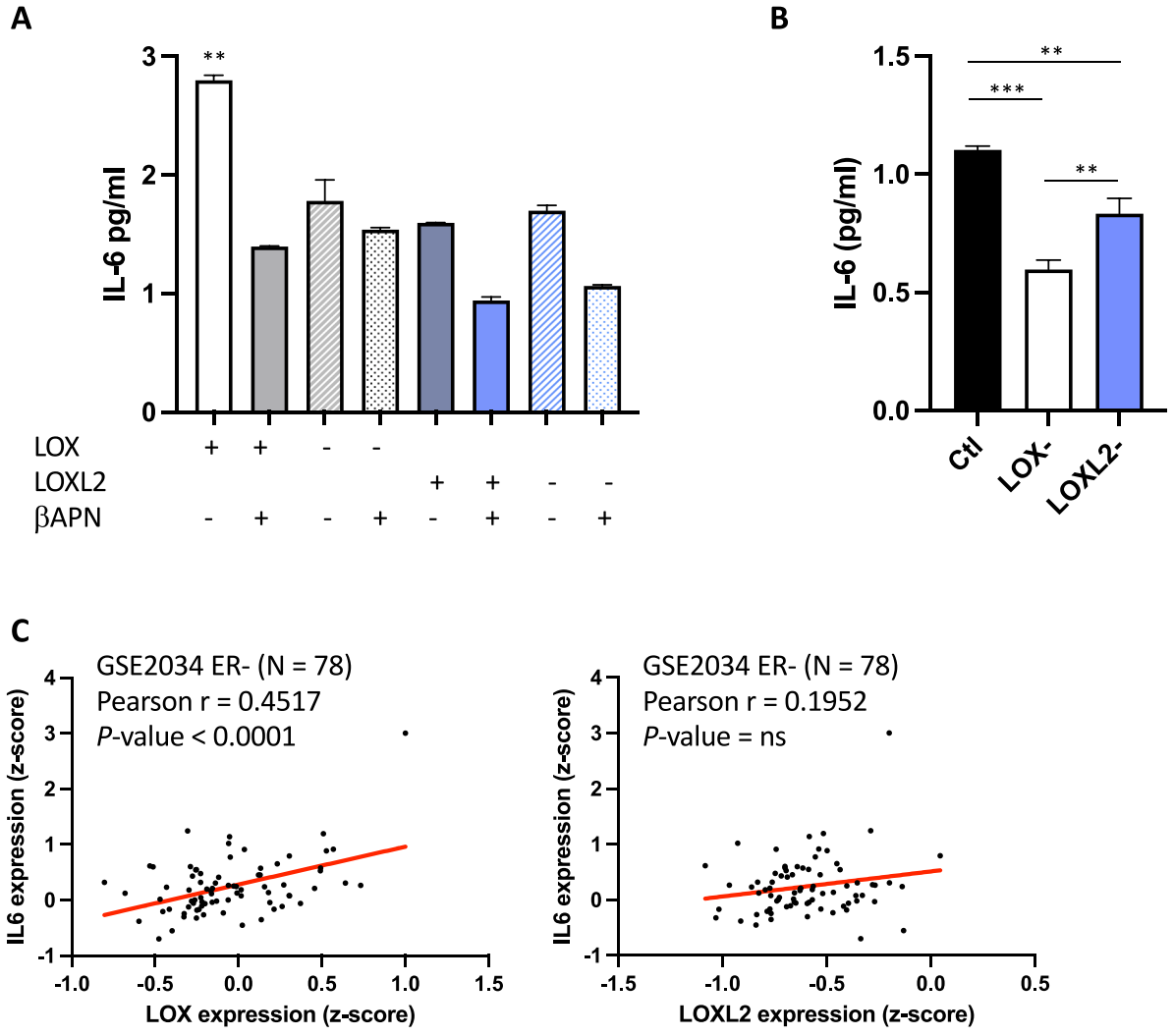

Fig. 6. LOX overexpression in breast cancer cells increases the production of the pro-osteoclastic cytokine IL-6. (A) ELISA measurement of IL-6 in the conditioned medium from +/− βAPN-treated B02 LOX(+), LOX(−), LOXL2(+) or LOXL2(−) cells. Data are the mean ± SD of three independent experiments. (B) ELISA measurement of IL-6 in the conditioned medium from MDA-MB-231 Ctrl, LOX(−), or LOXL2(−) cells. Data are the mean ± SD of three independent experiments. (C) Correlation between *IL-6* expression with that of *LOX* (left-hand panel) or *LOXL2* (right-hand panel) in ER-negative primary mammary tumors (n = 78) from a cohort of breast cancer patients (GSE2034). Pearson correlation coefficients and P-values obtained with the PRISM 9 software are indicated. **, ***: $p < 0.01$ and 0.001, respectively.

production, compared to that observed with *LOXL2* silencing (Fig. 6B). This link extended to the clinic because, as opposed to *LOXL2,* we observed a significant positive Pearson correlation between *LOX* and *IL-6* expression in ER-negative breast cancer (Fig. 6C and D). By contrast, *LOX* and *LOXL2* expression did not correlate with *IL-6* expression in ER-positive breast cancer (Supplementary Fig. S6).

5. Discussion

There is mounting evidence for a role of LOX and LOXL2 in facilitating breast cancer invasion and metastatic spread to visceral organs (lungs, liver) *in vivo* [1,3]. By contrast, the contribution of LOX and LOXL2 to breast cancer bone metastasis remains scant. In the present study, we found that LOX (but not LOXL2) promoted bone metastasis and bone destruction *in vivo*, and that LOX induced a robust expression of IL-6 in human triple negative breast cancer cells, whereas LOXL2 did not induce any change in IL-6 production by these tumor cells. In agreement with these data, LOX also stimulates IL-6 expression by fibroblasts in a pulmonary fibrosis model [17]. More importantly, IL-6 is a potent inflammatory cytokine that stimulates RANKL expression in bone cells and plays a key role in cancer growth and bone metastasis [19]. Here, tumor-secreted LOX (but not LOXL2) played a prominent role in enhancing RANKL-dependent differentiation of mature osteoclasts. It is also noteworthy that the stimulatory effects of LOX on *(i)* bone destruction *in vivo* (Figs. 2 and 3), *(ii)* IL-6 production and *(iii)* osteoclast differentiation *in vitro* (Figs. 4–6) were not compensated by other LOXL members since their expression levels in tumor cells were not modified by LOX overexpression or silencing (Supplementary Table S4). One limitation of our current study is that LOX-induced IL-6 expression was demonstrated using *in vitro* experiments only. However, we previously reported that LOX drives IL-6 production by human colorectal cancer cells *in vitro* and *in vivo*, and that LOX and IL-6 are acting in concert to promote osteoclast differentiation induced by RANKL [5]. Based on these previous findings [5] and current data, we propose a model in which LOX and IL-6 secreted from breast cancer cells also act in concert to enhance osteoclast-mediated bone resorption that, in turn, promotes metastatic bone destruction *in vivo*.

The reasons why tumor-derived LOXL2 did not promote osteoclast differentiation *in vitro* and bone destruction *in vivo* are unclear. LOXL2 produced by breast cancer cells was enzymatically active since the treatment of tumor cells with βAPN completely inhibited its catalytic activity (Fig. 1). Furthermore, the conditioned medium from MDA-MB-231 and Hs578T cells silenced for *LOXL2* significantly enhanced osteoclast differentiation (Fig. 5), suggesting that LOXL2 could negatively regulate endogenous LOX's pro-osteoclastic activity. Interestingly, the N-terminal pro-domains of LOXL2 contains SRCR domains that are thought to be involved in mediating protein–protein interactions [1,2], and LOXL3, *via* its SRCR-repeats, associates to signal transducer and activator of transcription 3 (STAT3) in the nucleus to inhibit its transcriptional activity in Hela cells [20]. In osteoclasts, STAT3 positively regulates the activity of NFATc1, which is a master regulator of osteoclastogenesis [21]. Moreover, we have previously shown that LOX promotes nuclear localization of NFATc1 in mature osteoclasts [5]. It is therefore conceivable that LOXL2 could negatively regulate LOX's pro-osteoclastic activity by binding to nuclear STAT3, thereby interfering with NFATc1 activity in osteoclasts. This hypothesis clearly warrants further investigation.

Surprisingly, neither breast cancer cell functions *in vitro* nor growth of subcutaneous tumor xenografts *in vivo* were affected by *LOX/LOXL2* silencing or overexpression. Nevertheless, our tumorigenesis data were in line with previous reports showing that LOX or LOXL2 is not required for primary mammary tumor growth and eventually reduces it, when using immunocompetent and immunocompromised orthotopic models (4T1 and MDA-MB-231, respectively) or a transgenic model (PyMT) of breast cancer [8,10,22]. For example, it has been shown that LOX/LOXL2 overexpression in 4T1 cells leads to a massive increase of central necrosis in tumor xenografts, thereby limiting their supply and subsequent tumor growth [23]. Interestingly, although *Loxl2* knockdown and *Loxl2*-overexpressing tumors are similar in size in the transgenic PyMT model, *Loxl2* knockdown tumors exhibit a more differentiated phenotype whereas *Loxl2*-overexpressing tumors have a less differentiated and more invasive phenotype than their corresponding controls [10]. These *in vivo* findings [10] are in line with the observation that LOX and LOXL2 activate key EMT transcription factors such as TWIST1, E47 and SNAIL2, which then promote the dedifferentiation of breast cancer cells and contribute to their invasiveness [6,23,24]. The reason why we did not observe any effect of LOX/LOXL2 on tumor cell functions may be because breast cancer cell lines (B02, MDA-MB-231 and Hs578T) used in our study are already mesenchymal and intrinsically highly invasive [16,25], thereby limiting the impact of LOX and LOXL2 on EMT and tumor cell motility/invasion. Similarly, B02, MDA-MB-231 and Hs578T cells already strongly attach and spread to collagen and fibronectin [25], which may have probably masked the stimulatory activity of LOX/LOXL2 on breast cancer cell adhesion to these extracellular matrix proteins. Moreover, in our *in vivo* model, we chose to inoculate LOX/LOXL2-engineered B02 cell lines directly into the bloodstream, thereby bypassing the invasive and intravasation processes, which are required steps for tumor cells to disseminate to distant organs. Thus, using these cell lines that already express EMT invasive markers we could focus on specific steps associated with bone metastasis to decipher the respective roles of LOX and LOXL2 during cancer-associated bone destruction.

6. Conclusion

Our findings collectively show that LOX and LOXL2 produced by triple negative breast cancer cells have distinct functions in breast cancer bone metastasis, without any cooperative or redundant roles. Indeed, LOX enhances bone resorption and subsequent destruction of bone during bone metastasis formation, whereas LOXL2 seems to counteract LOX's pro-osteoclastic activity. We believe this is crucially important information, which supports targeting specifically LOX for metastasis prevention, while therapeutic targeting of LOXL2 might potentially cause detrimental side effects by promoting bone destruction.

CRediT authorship contribution statement

Paola Di Mauro: Investigation, Methodology. **Martine Croset:** Investigation, Methodology. **Lamia Bouazza:** Methodology. **Philippe Clézardin:** Conceptualization, Funding acquisition, Project administration, Writing – review & editing. **Caroline Reynaud:** Conceptualization, Investigation, Methodology, Supervision, Writing – original draft.

Declaration of competing interest

The authors declare the following financial interests/personal relationships which may be considered as potential competing interests: Philippe Clezardin reports financial support was provided by Laboratoire d'Excellence DEVweCAN. Martine Croset reports financial support was provided by National Cancer Association (Ligue contre le Cancer). Caroline Reynaud reports financial support was provided by National Cancer Association (Ligue contre le Cancer). Philippe Clezardin reports a relationship with Amgen Inc that includes: consulting or advisory. JBO editorial board member (Philippe Clezardin). Other authors declare that they have no known competing financial interests or personal relationships that could have appeared to influence the work reported in this paper.

Acknowledgements

The technical support of Ms Soumaya El Moghrabi and Mr Jean-Paul Roux for bone histology and bone imaging, respectively, is gratefully acknowledged. We also acknowledge Dr Olivier Peyruchaud for valuable discussion.

Funding

CR and MC acknowledge the support of the Ligue contre le Cancer (Comité du Rhône). CR is supported by CNRS. PC is supported by INSERM, the University of Lyon, and the LabEX DEVweCAN (ANR-10-LABX-61) of Université de Lyon, within the program "Investissements d'Avenir" (ANR-11-IDEX-0007) operated by the French National Research Agency (ANR). PDM is a recipient of a PhD fellowship from the Ligue contre le Cancer.

Appendix A. Supplementary data

Supplementary data to this article can be found online at https://doi.org/10.1016/j.jbo.2024.100522.

References

[1] H.E. Barker, T.R. Cox, J.T. Erler, The rationale for targeting the LOX family in cancer, Nat. Rev. Cancer 12 (2012) 540–552, https://doi.org/10.1038/nrc3319.
[2] V.G. Martínez, S.K. Moestrup, U. Holmskov, J. Mollenhauer, F. Lozano, The conserved scavenger receptor cysteine-rich superfamily in therapy and diagnosis, Pharmacol. Rev. 63 (2011) 967–1000, https://doi.org/10.1124/pr.111.004523.
[3] W. Wang, X. Wang, F. Yao, C. Huang, Lysyl oxidase family proteins: prospective therapeutic targets in Cancer, Int. J. Mol. Sci. 23 (2022) 12270, https://doi.org/10.3390/ijms232012270.
[4] F. Pez, F. Dayan, J. Durivault, B. Kaniewski, G. Aimond, G.S. Le Provost, B. Deux, P. Clézardin, P. Sommer, J. Pouysségur, C. Reynaud, The HIF-1-inducible lysyl oxidase activates HIF-1 via the Akt pathway in a positive regulation loop and synergizes with HIF-1 in promoting tumor cell growth, Cancer Res. 71 (2011) 1647–1657, https://doi.org/10.1158/0008-5472.CAN-10-1516.
[5] C. Reynaud, L. Ferreras, P. Di Mauro, C. Kan, M. Croset, E. Bonnelye, F. Pez, C. Thomas, G. Aimond, A.E. Karnoub, M. Brevet, P. Clézardin, Lysyl oxidase is a strong determinant of tumor cell colonization in bone, Cancer Res. 77 (2017) 268–278, https://doi.org/10.1158/0008-5472.CAN-15-2621.
[6] M. Boufraqech, L. Zhang, N. Nilubol, S.M. Sadowski, S. Kotian, M. Quezado, E. Kebebew, Lysyl oxidase (LOX) transcriptionally regulates SNAI2 expression and TIMP4 secretion in human cancers, Clin. Cancer Res. 22 (2016) 4491–4504, https://doi.org/10.1158/1078-0432.
[7] V. Barry-Hamilton, R. Spangler, D. Marshall, S. McCauley, H.M. Rodriguez, M. Oyasu, A. Mikels, M. Vaysberg, H. Ghermazien, C. Wai, C.A. Garcia, A. C. Velayo, B. Jorgensen, D. Biermann, D. Tsai, J. Green, S. Zaffryar-Eilot, A. Holzer, S. Ogg, D. Thai, G. Neufeld, P. Van Vlasselaer, V. Smith, Allosteric inhibition of lysyl oxidase-like-2 impedes the development of a pathologic microenvironment, Nat. Med. 16 (2010) 1009–1017, https://doi.org/10.1038/nm.2208.
[8] H.E. Barker, J. Chang, T.R. Cox, G. Lang, D. Bird, M. Nicolau, H.R. Evans, A. Gartland, J.T. Erler, LOXL2-mediated matrix remodeling in metastasis and mammary gland involution, Cancer Res. 71 (2011) 1561–1572, https://doi.org/10.1158/0008-5472.CAN-10-2868.
[9] C. Rachman-Tzemah, S. Zaffryar-Eilot, M. Grossman, D. Ribero, M. Timaner, J. M. Mäki, J. Myllyharju, F. Bertolini, D. Hershkovitz, I. Sagi, P. Hasson, Y. Shaked, Cell Rep. 25 (2017) 774–784, https://doi.org/10.1016/j.celrep.2017.04.005.
[10] F. Salvador, A. Martin, C. López-Menéndez, G. Moreno-Bueno, V. Santos, A. Vázquez-Naharro, P.G. Santamaria, S. Morales, P.R. Dubus, L. Muinelo-Romay, R. López-López, J.C. Tung, V.M. Weaver, F. Portillo, A. Cano, Lysyl Oxidase-like Protein LOXL2 promotes lung metastasis of breast cancer, Cancer Res. 77 (2017) 5846–5859, https://doi.org/10.1158/0008-5472.CAN-16-3152.
[11] Q. Li, C.C. Zhu, B. Ni, Z.Z. Zhang, S.H. Jiang, L.P. Hu, X. Wang, X.X. Zhang, P. Q. Huang, Q. Yang, J. Li, J.R. Gu, J. Xu, K.Q. Luo, G. Zhao, Z.G. Zhang, Lysyl oxidase promotes liver metastasis of gastric cancer via facilitating the reciprocal interactions between tumor cells and cancer associated fibroblasts, EBioMedicine 49 (2019) 157–171, https://doi.org/10.1016/j.ebiom.2019.10.037.
[12] M. Tsukasaki, K. Hamada, K. Okamoto, K. Nagashima, A. Terashima, N. Komatsu, S.J. Win, T. Okamura, T. Nitta, H. Yasuda, J.M. Penninger, H. Takayanagi, LOX fails to substitute for RANKL in osteoclastogenesis, J. Bone Miner. Res. 32 (2017) 434–439, https://doi.org/10.1002/jbmr.2990.
[13] O. Peyruchaud, B. Winding, I. Pécheur, C.M. Serre, P. Delmas, P. Clézardin, Early detection of bone metastases in a murine model using fluorescent human breast cancer cells: application to the use of the bisphosphonate zoledronic acid in the treatment of osteolytic lesions, J. Bone Miner. Res. 16 (2001) 2027–2034, https://doi.org/10.1359/jbmr.2001.16.11.2027.
[14] M. Croset, F. Pantano, C.W.S. Kan, E. Bonnelye, F. Descotes, C. Alix-Panabières, C. H. Lecellier, R. Bachelier, N. Allioli, S.S. Hong, K. Bartkowiak, K. Pantel, P. Clézardin, miRNA-30 family members inhibit breast cancer invasion, osteomimicry, and bone destruction by directly targeting multiple bone metastasis-associated genes, Cancer Res. 78 (2018) 5259–5273, https://doi.org/10.1158/0008-5472.CAN-17-3058.
[15] M. Croset, D. Goehrig, A. Frackowiak, E. Bonnelye, S. Ansieau, A. Puisieux, P. Clézardin, TWIST1 expression in breast cancer cells facilitates bone metastasis formation, J. Bone Miner. Res. 29 (2014) 1886–1899, https://doi.org/10.1002/jbmr.2215.
[16] A. Fradet, H. Sorel, L. Bouazza, D. Goehrig, B. Dépalle, A. Bellahcène, V. Castronovo, H. Follet, F. Descotes, J.E. Aubin, P. Clézardin, E. Bonnelye, Dual function of ERRα in breast cancer and bone metastasis formation: implication of VEGF and osteoprotegerin, Cancer Res. 71 (2011) 5728–5738, https://doi.org/10.1158/0008-5472.CAN-11-1431.
[17] X.X. Nguyen, T. Nishimoto, T. Takihara, L. Mlakar, A.D. Bradshaw, C. Feghali-Bostwick, Lysyl oxidase directly contributes to extracellular matrix production and fibrosis in systemic sclerosis, Am. J. Physiol. Lung Cell. Mol. Physiol. 320 (2021) L29–L40, https://doi.org/10.1152/ajplung.00173.2020.
[18] A. Teti, S. Migliaccio, A. Taranta, L. Mlakar, S. Bernardini, G. De Rossi, M. Luciani, M. Iacobini, L. De Felice, R. Boldrini, C. Bosman, A. Corsi, P. Bianco, Mechanisms of osteoclast dysfunction in human osteopetrosis: abnormal osteoclastogenesis and lack of osteoclast-specific adhesion structures, J. Bone Miner. Res. 14 (1999) 2007–2017, https://doi.org/10.1359/jbmr.1999.14.12.2107.
[19] P. Clézardin, R. Coleman, M. Puppo, P. Ottewell, E. Bonnelye, F. Paycha, C. B. Confavreux, I. Holen, Bone metastasis: mechanisms, therapies, and biomarkers, Physiol. Rev. 101 (2021) 797–855, https://doi.org/10.1152/physrev.00012.2019.
[20] L. Ma, C. Huang, X.J. Wang, D.E. Xin, L.S. Wang, Q.C. Zou, Y.S. Zhang, M.D. Tan, Y. M. Wang, T.C. Zhao, D. Chatterjee, R.A. Altura, C. Wang, Y.S. Xu, J.H. Yang, Y. S. Fan, B.H. Han, J. Si, X. Zhang, J. Cheng, Z. Chang, Y.E. Chin, Lysyl oxidase 3 is a dual-specificity enzyme involved in STAT3 deacetylation and deacetylimination modulation, Mol. Cell. 65 (2017) 296–309, https://doi.org/10.1016/j.molcel.2016.12.002.
[21] Y. Yang, M.R. Chung, S. Zhou, X. Gong, H. Xu, Y. Hong, A. Jin, X. Huang, W. Zou, Q. Dai, L. Jiang, STAT3 controls osteoclast differentiation and bone homeostasis by regulating NFATc1 transcription, J. Biol. Chem. 294 (2019) 15395–15407, https://doi.org/10.1074/jbc.RA119.010139.
[22] L. Rossow, S. Veitl, S. Vorlová, J.K. Wax, A.E. Kuhn, V. Maltzahn, B. Upcin, F. Karl, H. Hoffmann, S. Gätzner, M. Kallius, R. Nandigama, D. Scheld, S. Irmak, S. Herterich, A. Zernecke, S. Ergün, E. Henke, LOX-catalyzed collagen stabilization is a proximal cause for intrinsic resistance to chemotherapy, Oncogene 37 (2018) 4921–4940, https://doi.org/10.1038/s41388-018-0320-2.
[23] C.P. El-Haibi, G.W. Bell, J. Zhang, A.Y. Collmann, D. Wood, C.M. Scherber, et al., Critical role for lysyl oxidase in mesenchymal stem cell-driven breast cancer malignancy, Proc. Natl. Acad. Sci. U.S.A. 109 (2012) 17460–17465.
[24] G. Canesin, E.P. Cuevas, V. Santos, C. López-Menéndez, G. Moreno-Bueno, Y. Huang, K. Csiszar, F. Portillo, H. Peinado, D. Lyden, A. Cano, Lysyl oxidase-like 2 (LOXL2) and E47 EMT factor: novel partners in E-cadherin repression and early metastasis colonization, Oncogene 34 (2015) 951–964, https://doi.org/10.1038/onc.2014.23.
[25] F. Pantano, M. Croset, K. Driouch, N. Bednarz-Knoll, M. Iuliani, G. Ribelli, E. Bonnelye, H. Wikman, S. Geraci, F. Bonin, S. Simonetti, B. Vincenzi, S.S. Hong, S. Sousa, K. Pantel, G. Tonini, D. Santini, P. Clézardin, Integrin alpha5 in human breast cancer is a mediator of bone metastasis and a therapeutic target for the treatment of osteolytic lesions, Oncogene 40 (2021) 1284–1299, https://doi.org/10.1038/s41388-020-01603-6.